



Title	Rapid screening of antineoplastic candidates for the human organic anion transporter OATP1B3 substrates using fluorescent probes
Author(s)	Yamaguchi, Hiroaki; Kobayashi, Minako; Okada, Masahiro; Takeuchi, Toshiko; Unno, Michiaki; Abe, Takaaki; Goto, Junichi; Hishinuma, Takanori; Mano, Nariyasu
Citation	Cancer Letters, 260(1-2), 163-169 https://doi.org/10.1016/j.canlet.2007.10.040
Issue Date	2008-02-18
Doc URL	http://hdl.handle.net/2115/43859
Type	article (author version)
File Information	yamaguchi2008.pdf



[Instructions for use](#)

Rapid screening of antineoplastic candidates for the human organic anion transporter OATP1B3 substrates using fluorescent probes

Hiroaki Yamaguchi^{1,2}, Minako Kobayashi², Masahiro Okada², Toshiko Takeuchi², Michiaki Unno³, Takaaki Abe^{4,5}, Junichi Goto ^{1,2}, Takanori Hishinuma⁶, Nariyasu Mano^{1,2,7}

From ¹ Department of Pharmaceutical Sciences, Tohoku University Hospital, Sendai, Japan, ²Division of Clinical Pharmacy, Graduate School of Pharmaceutical Sciences, Tohoku University, Sendai, Japan, ³Division of Gastroenterological Surgery, Department of Surgery, Tohoku University Graduate School of Medicine, Japan, ⁴Division of Nephrology, Endocrinology, and Vascular Medicine, Department of Medicine, Tohoku University Graduate School of Medicine, Sendai, Japan, ⁵PRESTO, Japan Science and Technology Corporation, Japan, and ⁶Division of Pharmacotherapy, Graduate School of Pharmaceutical Sciences, Tohoku University, Sendai, Japan

⁷Address correspondence to: Nariyasu Mano, Ph.D., Department of Pharmaceutical Sciences, Tohoku University Hospital, 1-1 Seiryomachi, Aoba-ku, Sendai 980-8574, Japan. Phone: +81-22-717-7525; FAX: +81-22-717-7545; E-mail: n-mano@mail.tains.tohoku.ac.jp

Abstract

A rapid screening system has been established to extract novel candidates that exhibit potent inhibition of the transport of fluorescent substrate by organic anion transporting polypeptide (OATP) 1B3. OATP1B3 is abundantly expressed in solid digestive organ cancers. Thus, the identification of new substrates leads to novel strategies for effective cancer chemotherapy with minimal adverse effects. We used an automated image acquisition and analysis system (IN Cell Analyzer 1000) to visualize the transport and subsequent accumulation of the fluorescent substrate chenodeoxycholy-(N ϵ -NBD)-lysine (CDCA-NBD). Antineoplastic screening demonstrated that five candidate agents, docetaxel, actinomycin D, mitoxantrone, paclitaxel, and SN-38, exhibited potent inhibitory effects on OATP1B3-mediated transport of CDCA-NBD. To clarify if these antineoplastic drugs are substrates for OATP1B3, we performed transport assays in OATP1B3-expressing cells. We determined that SN-38 is a novel substrate for OATP1B3. In conclusion, our results demonstrate that the screening system established in this study is a useful method for the rapid extraction of candidate therapeutic agents from the large numbers of compounds.

Keywords: antineoplastic drugs, fluorescent substrate, imaging, OATP1B3, and rapid screening

Introduction

Organic anion transporting polypeptides (OATPs) are sodium-independent organic anion transporters expressed in a wide variety of tissues, including the liver, kidney, intestine, and brain. OATPs contribute to the transport of bile acids, thyroid hormones, steroid conjugates, anionic oligopeptides, eicosanoids, drugs, and other xenobiotic compounds across membranes [1-4]. OATP1B3 (LST-2/OATP8), a member of the liver-specific subfamily of OATPs, localizes to the basolateral membrane of hepatocytes [5-8]. OATP1B3 is also expressed by solid digestive organ neoplasms, including gastric, pancreatic, and colon cancers [7]. OATP1B3 is weakly expressed by the normal liver, but strongly upregulated by cancer cells. Thus, a greater understanding of the interaction between OATP1B3 and antineoplastic drugs would be useful to develop novel strategies for effective cancer chemotherapeutics with minimal adverse effects.

Fluorescent bile acids are efficiently transported by both OATP1B1 and OATP1B3 [9]. We have recently succeeded in the visualization of the transport process using confocal imaging. We applied this imaging technique to the screening of transporter substrates. In this study, we examined the effects of antineoplastic drugs on the transport of fluorescent substrates via OATP1B3 using an automated image acquisition and analysis system (IN Cell Analyzer 1000). We have discovered a new substrate for OATP1B3, suggesting that this system can be instrumental in the rapid screening of novel candidate substrates.

Materials and Methods

Materials

Chenodeoxycholy-(N ϵ -NBD)-lysine (CDCA-NBD) was synthesized as previously described [9]. Anti-OATP8 antibody was purchased from Affinity BioReagents, Inc. (Golden, CO). All other chemicals were commercially available and of the highest purity possible.

Cell culture and transfection studies

HEK293 cells, which are derived from human embryonic kidneys, were cultured in Dulbecco's modified Eagle's medium supplemented with 10% fetal bovine serum in an atmosphere of 5% CO₂, 95% air at 37°C. Cells were transfected with a pcDNA3.1(+) plasmid vector (Invitrogen) encoding OATP1B3 using LipofectAMINE 2000 (Invitrogen) according to the manufacturer's instructions. After three weeks of selection in G418 (0.5 mg/mL), we screened single colonies for OATP1B3 expression by immunoblot analysis and transport studies. Cells transfected with empty vector (HEK/pcDNA3.1(+)) were used as controls.

Immunoblot analysis.

Membrane fractions (15 μ g/lane) were separated by SDS-polyacrylamide gel electrophoresis (8%). OATP1B3 was detected with a monoclonal anti-OATP8 antibody diluted 1:100, and detection was performed using Peroxidase-conjugated AffiniPure Goat Anti-Mouse IgG+IgM (H+L) (Jackson ImmunoResearch, West Grove, PA) diluted 1:10000.

Transport study.

We measured the cellular uptake of CDCA-NBD in monolayer cultures grown on 24-well plates. After washing once, cells were preincubated in Krebs–Henseleit buffer (118 mM NaCl, 23.8 mM NaHCO₃, 4.83 mM KCl, 0.96 mM KH₂PO₄, 1.20 mM MgSO₄, 12.5 mM HEPES, 5.0 mM glucose, and 1.53 mM CaCl₂, pH 7.4). Uptake was initiated by adding CDCA-NBD to the medium. At the indicated times, uptake was terminated by replacement of the uptake buffer

with ice-cold Krebs-Henseleit buffer containing 1% BSA. After washing two times in ice-cold BSA-free Krebs-Henseleit buffer, cells were lysed in lysis buffer (20 mM Tris with 0.4% Triton X-100, adjusted to pH 9.0). The fluorescence contained in each aliquot was measured using a microplate spectrofluorometer (SPECTRAmax GEMINI XS; Molecular Devices, Sunnyvale, CA) at an excitation wavelength of 485 nm and an emission wavelength of 538 nm.

Similarly, uptake of actinomycin D, mitoxantrone, and SN-38 were determined. Uptake of actinomycin D was measured by the fluorescence at an excitation wavelength of 360 nm and an emission wavelength of 480 nm. Mitoxantrone was determined at an excitation wavelength of 623 nm and an emission wavelength of 690 nm, and SN-38 was determined at an excitation wavelength of 380 nm and an emission wavelength of 540 nm

We measured the uptake of docetaxel and paclitaxel by monolayer cultures grown in six-well plates using high-performance liquid chromatography (HPLC). After terminating antineoplastic drug uptake, cells were scraped and homogenized in 1 mL of water. Known quantities of paclitaxel or docetaxel were added to each cell lysate sample as an internal standard. Antineoplastic drugs were extracted using 3-mL Bond Elut C18 cartridges (Varian, Harbor City, CA). The HPLC system consisted of a Nanospace SI-1 (Shiseido, Tokyo, Japan) equipped with an ultraviolet ray detector set at 230 nm. Chromatography utilized isocratic elution from a C18 Capcell Pak UG120 column (Shiseido; 1.5 × 150 mm, 5 μm) in acetonitrile–water (50:50, vol/vol, pH 4.0 with acetic acid) at a flow rate of 100 μL/min.

The protein content of the solubilized cells was determined using a Protein Assay kit (Bio-Rad Laboratories Inc., Hercules, CA).

Screening of antineoplastic drugs

Cells seeded in 96-well plates (8×10^3 cells/well) were incubated for 24 hours. Cell nuclei were stained with 100 μL Hoechst 33258 (Sigma, St. Louis, MO) solution (20 μM in DMEM)

for 20 minutes in a 5% CO₂, 95% air atmosphere at 37°C. Cells were washed once after nuclear staining, then preincubated in Krebs–Henseleit buffer for 10 minutes. Uptake was initiated by the addition of CDCA-NBD (0.1 μM) in the presence or absence of antineoplastic drugs (5 or 20 μM). BSP (bromosulfophtalein), a representative OATP1B3 substrate, was used as a positive control. After 20 minutes of uptake, we measured CDCA-NBD and Hoechst 33258 fluorescence intensity using an automated image acquisition and analysis system (IN Cell Analyzer 1000, GE Healthcare) at excitation wavelengths of 460 and 360 nm and emission wavelengths of 535 and 475 nm, respectively. Fluorescence intensities were analyzed using the "Object Intensity Module" of the IN Cell Analyzer 1000 [10].

Statistical analysis.

Data are expressed as means ± S.E. When appropriate, the differences between groups were tested for significance using the unpaired Student's *t* test. Statistical significance was indicated by *P* values less than 0.05.

Results

Transport of CDCA-NBD by OATP1B3-transfected cells

First, we established stable clones overproducing OATP1B3. Clones that survived selection in 0.5 mg/mL G418 were expanded. Analysis for OATP1B3 overproduction by immunoblotting and CDCA-NBD uptake (Fig. 1A and 1B) isolated two clones, OATP1B3-9 and OATP1B3-10. OATP1B3-9 exhibited higher expression levels and transport activity of OATP1B3 than OATP1B3-10 (Fig. 1B). Kinetic parameters in OATP1B3-9 were determined after exposure to varying concentrations of CDCA-NBD (Fig. 1C). The apparent Michaelis-Menten constant (K_m) for OATP1B3-mediated CDCA-NBD uptake was 0.53 ± 0.17 μM , and the maximum velocity (V_{max}) was 279 ± 117 pmol/mg protein/min. This result is consistent with previous data using HepG2 cells with transient expression of OATP1B3 [9]. OATP1B3-mediated CDCA-NBD transport was also reduced by several previously reported substrates (inhibitors) (Fig. 1D).

Screening of antineoplastic drugs in OATP1B3-transfected cells

In this study, we examined the effects of antineoplastic drugs on OATP1B3-mediated transport of fluorescent substrates using an IN Cell Analyzer 1000 system. CDCA-NBD, which is efficiently transported by OATP1B3, was used as a fluorescent probe. Eighteen antineoplastic drugs with a variety of mechanisms of action were selected; BSP was used as a positive control. CDCA-NBD fluorescence intensity was measured using the IN Cell Analyzer 1000 (Fig. 2). The result of screening, three and nine antineoplastic drugs significantly inhibited CDCA-NBD transport at inhibitory concentrations of 5 and 20 μM , respectively (Table 1). At higher inhibitory concentrations (20 μM), docetaxel, actinomycin D, mitoxantrone, paclitaxel, and SN-38 inhibited transport to a greater extent than methotrexate, a reported OATP1B3 substrate, and decreased the observed fluorescent intensities to 27, 61,

54, 50, and 49%, respectively.

Transport of antineoplastic drugs by OATP1B3-expressing cells

We examined the uptake study to clarify whether these five neoplastic agents were OATP1B3 substrates. SN-38 alone demonstrated significant transport by OATP1B3-expressing HEK293 cells (Fig. 3). The other drugs were not significantly transported.

Discussion

In this study, we developed a screening system to extract antineoplastic candidates that are OATP1B3 substrates using an automated image acquisition and analysis system (IN Cell Analyzer 1000). As OATP1B3 is abundantly expressed in liver and other solid digestive organ cancers [7], effective cancer chemotherapy could exploit the OATP1B3 protein to allow the increased accumulation of antineoplastic drugs in cancer cells.

CDCA-NBD is a fluorescent probe that is efficiently transported by OATP1B3 (Fig. 1) [9]. We are able to visualize the uptake of CDCA-NBD in living cells (Fig. 2). Our initial screening revealed several potent inhibitors of CDCA-NBD uptake (docetaxel, actinomycin D, mitoxantrone, paclitaxel, and SN-38) (Table 1). This result indicated that our novel screening system is highly informative. Interestingly, vinblastine and vincristine increased the uptake of CDCA-NBD. This result looks similar to the previous result of increased methotrexate uptake induced by vinblastine and vincristine [11]. It is possible that some of substrates for OATP1B3 are *cis*-stimulated by vinblastine and vincristine.

It is important to identify if each extracted antineoplastic candidate is a substrate for OATP1B3. We therefore examined uptake studies, in which candidate transport into the cells is directly measured (Fig. 3). SN-38 was significantly transported into OATP1B3-9 cells. OATP1B3-9 cells were more sensitive to SN-38 than mock cells by cytotoxicity assay (IC_{50} value; 2.35 ± 0.45 for OATP1B3-9 and 3.92 ± 0.38 nM for mock cells, $n = 4$, $P < 0.05$). This is the first report that SN-38 is a substrate for OATP1B3. Previous reports have demonstrated that SN-38 is a substrate for OATP1B1, but not OATP1B3, which is inconsistent with our results [12]. In some case, different expression system for transporter protein makes different results. For example, taurocholic acid is reported to be a substrate for OATP1B3 using *Xenopus leavis* oocyte system but not a substrate using HEK293 system [7, 13]. The

reason for these discrepancies is unclear. We could not, however, observe substantial transport of paclitaxel, docetaxel, mitoxantrone, or actinomycin D by OATP1B3-9 cells. Paclitaxel and docetaxel are reported to be substrates for OATP1B3 in the *Xenopus leavis* oocytes expression system [8]. The discrepancy may result from differences in the transporter expression system.

In conclusion, we established a rapid screening using a fluorescent probe system to evaluate large numbers of antineoplastic candidates. From our screening results, this system is capable of identifying novel substrates for OATP1B3. Our results suggest that this screening system is useful for the rapid and exact extraction of the candidates from enormous numbers of compounds.

Acknowledgments

This work was supported in part by a grant from the Ministry of Education, Culture, Sports, Science and Technology of Japan.

References

- [1] B. Hagenbuch, P.J. Meier, Organic anion transporting polypeptides of the OATP/ SLC21 family: phylogenetic classification as OATP/ SLCO superfamily, new nomenclature and molecular/functional properties, *Pflugers Arch* 447 (2004) 653-665
- [2] T. Mikkaichi, T. Suzuki, M. Tanemoto, S. Ito, T. Abe, The organic anion transporter (OATP) family, *Drug Metab Pharmacokinet* 19 (2004) 171-179
- [3] B. Hagenbuch, P.J. Meier, The superfamily of organic anion transporting polypeptides, *Biochim Biophys Acta* 1609 (2003) 1-18
- [4] G.A. Kullak-Ublick, B. Stieger, P.J. Meier, Enterohepatic bile salt transporters in normal physiology and liver disease, *Gastroenterology* 126 (2004) 322-342
- [5] J. Konig, Y. Cui, A.T. Nies, D. Keppler, Localization and genomic organization of a new hepatocellular organic anion transporting polypeptide, *J Biol Chem* 275 (2000) 23161-23168
- [6] Y. Cui, J. Konig, A.T. Nies, M. Pfannschmidt, M. Hergt, W.W. Franke, W. Alt, R. Moll, D. Keppler, Detection of the human organic anion transporters SLC21A6 (OATP2) and SLC21A8 (OATP8) in liver and hepatocellular carcinoma, *Lab Invest* 83 (2003) 527-538
- [7] T. Abe, M. Unno, T. Onogawa, T. Tokui, T.N. Kondo, R. Nakagomi, H. Adachi, K. Fujiwara, M. Okabe, T. Suzuki, K. Nunoki, E. Sato, M. Kakyo, T. Nishio, J. Sugita, N. Asano, M. Tanemoto, M. Seki, F. Date, K. Ono, Y. Kondo, K. Shiiba, M. Suzuki, H. Ohtani, T. Shimosegawa, K. Iinuma, H. Nagura, S. Ito, S. Matsuno, LST-2, a human liver-specific organic anion transporter, determines methotrexate sensitivity in gastrointestinal cancers, *Gastroenterology* 120 (2001) 1689-1699
- [8] N.F. Smith, M.R. Acharya, N. Desai, W.D. Figg, A. Sparreboom, Identification of OATP1B3 as a high-affinity hepatocellular transporter of paclitaxel, *Cancer Biol Ther* 4 (2005) 815-818
- [9] H. Yamaguchi, M. Okada, S. Akitaya, H. Ohara, T. Mikkaichi, H. Ishikawa, M. Sato, M. Matsuura, T. Saga, M. Unno, T. Abe, N. Mano, T. Hishinuma, J. Goto, Transport of fluorescent chenodeoxycholic acid via the human organic anion transporters OATP1B1 and OATP1B3, *J Lipid Res* 47 (2006) 1196-1202
- [10] P. Ramm, Y. Alexandrov, A. Cholewinski, Y. Cybuch, R. Nadon, B.J. Soltys, Automated screening of neurite outgrowth, *J Biomol Screen* 8 (2003) 7-18
- [11] M.J. Fyfe, I.D. Goldman, Characteristics of the vincristine-induced augmentation of methotrexate uptake in Ehrlich ascites tumor cells, *J Biol*

Chem 248 (1973) 5067-5073

- [12] T. Nozawa, H. Minami, S. Sugiura, A. Tsuji, I. Tamai, Role of organic anion transporter OATP1B1 (OATP-C) in hepatic uptake of irinotecan and its active metabolite, 7-ethyl-10-hydroxycamptothecin: in vitro evidence and effect of single nucleotide polymorphisms, *Drug Metab Dispos* 33 (2005) 434-439
- [13] Y. Cui, J. Konig, I. Leier, U. Buchholz, D. Keppler, Hepatic uptake of bilirubin and its conjugates by the human organic anion transporter SLC21A6, *J Biol Chem* 276 (2001) 9626-9630

Figure legends

Figure 1 Characteristics of CDCA-NBD uptake in cells stably transfected with OATP1B3. (A) Immunoblot analysis of OATP1B3. (B) Time course of CDCA-NBD uptake. OATP1B3-9 cells (closed circle), OATP1B3-10 cells (closed triangle), or mock cells (open circle) were incubated at 37°C for the indicated times with 0.5 μ M CDCA-NBD. Each point represents the mean \pm S.E. of three independent determinations. (C) Concentration-dependent uptake of CDCA-NBD by OATP1B3. Cells were incubated for 1 min at 37°C with varying concentrations of CDCA-NBD. We calculated OATP1B3-mediated uptake after subtracting the nonspecific uptake by mock cells. Each point represents the mean \pm S.E. of three independent experiments. (D) Inhibition of CDCA-NBD uptake. Cells were incubated at 37°C for 1 min with 0.5 μ M CDCA-NBD in the absence or presence of the indicated compounds. OATP1B3-mediated uptake was calculated by subtracting the nonspecific uptake by mock cells. Data are expressed as percentages of the control values. Each column represents the mean \pm S.E. of three to six independent experiments. * P < 0.05, significantly different from control. BSP, bromosulphophthalein; T₄, thyroxine; T₃, triiodothyronine; E3S, estrone-3-sulfate; CsA, cyclosporin A.

Figure 2 Screening of antineoplastic candidates. Images of nuclear staining (A) and CDCA-NBD uptake (B) in the presence or absence (control) of antineoplastic drugs (5 or 20 μ M) are shown.

1, 5-Fluorouracil; 2, Cytarabine; 3, 6-Mercaptopurine; 4,

2-Chloro-2'-deoxyadenosine; 5, Vinblastine; 6, Gemcitabine; 7, Vincristine; 8,

Docetaxel; 9, Actinomycin D; 10, Carboplatin; 11,
2-Fluoroadenine-9- β -D-arabinofuranoside; 12, Mitoxantrone; 13, Camptothecin;
14, Methotrexate; 15, Mitomycin C; 16, Paclitaxel; 17, Irinotecan; 18, SN-38

Figure 3 Uptake of antineoplastic candidates by OATP1B3. OATP1B3-10 cells (closed circle) or mock cells (open circle) were incubated at 37°C for the indicated periods with 5 μ M docetaxel (A), actinomycin D (B), mitoxantrone (C), paclitaxel (D), or SN-38 (E). Each point represents the mean \pm S.E. of three independent experiments. * $P < 0.05$, significantly different from the uptake by mock cells.

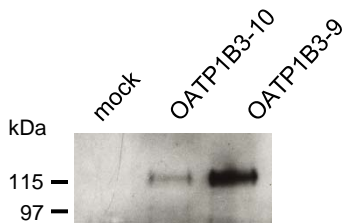
Table 1 Inhibitory effect of various antineoplastic drugs on OATP1B3-mediated CDCA-NBD uptake.

Inhibitor	5 μ M				20 μ M			
	N _{mock} (events)	N _{OATP1B3} (events)	Intensity (OATP1B3-mock)	Uptake (%)	N _{mock} (events)	N _{OATP1B3} (events)	Intensity (OATP1B3-mock)	Uptake (%)
Control	14 (88 \pm 35)	14 (81 \pm 24)	139 \pm 17	100.0	14 (59 \pm 44)	14 (71 \pm 32)	118 \pm 16	100.0
5-Fluorouracil	13 (92 \pm 51)	13 (76 \pm 21)	145 \pm 17	106.3 \pm 3.6	14 (70 \pm 34)	14 (76 \pm 39)	111 \pm 17	82.4 \pm 4.9 *
Cytarabine	14 (81 \pm 41)	14 (81 \pm 14)	132 \pm 15	104.6 \pm 5.6	13 (69 \pm 45)	13 (82 \pm 28)	129 \pm 19	98.0 \pm 5.2
6-Mercaptopurine	14 (98 \pm 80)	14 (79 \pm 28)	127 \pm 14	101.1 \pm 4.9	13 (84 \pm 36)	13 (80 \pm 20)	144 \pm 18	107.7 \pm 4.6
2-Chloro-2'-deoxyadenosine	13 (93 \pm 42)	13 (81 \pm 25)	133 \pm 16	103.3 \pm 5.2	13 (64 \pm 37)	13 (66 \pm 24)	116 \pm 16	87.8 \pm 4.9 *
Vinblastine	14 (80 \pm 32)	14 (83 \pm 24)	174 \pm 21	133.9 \pm 7.7	14 (71 \pm 30)	14 (71 \pm 33)	149 \pm 18	115.4 \pm 6.6
Gemcitabine	14 (81 \pm 50)	14 (80 \pm 17)	134 \pm 15	105.8 \pm 6.6	14 (74 \pm 39)	14 (80 \pm 30)	121 \pm 15	94.5 \pm 5.0
Vincristine	13 (82 \pm 41)	13 (68 \pm 23)	114 \pm 13	90.0 \pm 4.4	14 (44 \pm 32)	14 (74 \pm 29)	198 \pm 25	156.1 \pm 14.9
Docetaxel	14 (74 \pm 42)	14 (78 \pm 18)	108 \pm 19	81.9 \pm 11.1	14 (56 \pm 57)	14 (66 \pm 36)	36 \pm 7	26.5 \pm 3.8 *
Actinomycin D	14 (90 \pm 46)	14 (82 \pm 22)	115 \pm 13	90.0 \pm 5.8	14 (51 \pm 42)	14 (73 \pm 35)	80 \pm 10	61.2 \pm 3.9 *
Carboplatin	12 (73 \pm 39)	12 (81 \pm 15)	123 \pm 18	94.7 \pm 4.6	14 (70 \pm 32)	14 (82 \pm 32)	129 \pm 17	98.9 \pm 4.5
2-Fluoroadenine-9- β -D-Arabinofuranoside	13 (83 \pm 43)	13 (70 \pm 19)	130 \pm 16	96.6 \pm 6.0	13 (84 \pm 32)	13 (89 \pm 30)	136 \pm 20	101.5 \pm 5.8
Mitoxantrone	13 (70 \pm 48)	13 (76 \pm 22)	113 \pm 13	80.8 \pm 6.4 *	13 (51 \pm 53)	13 (70 \pm 38)	69 \pm 10	53.7 \pm 3.4 *
Camptothecin	10 (73 \pm 36)	10 (77 \pm 28)	91 \pm 23	85.3 \pm 6.8 *	10 (24 \pm 18)	10 (74 \pm 36)	110 \pm 21	99.4 \pm 4.3
Methotrexate	13 (94 \pm 52)	13 (79 \pm 15)	113 \pm 14	94.6 \pm 5.3	12 (78 \pm 32)	12 (71 \pm 35)	103 \pm 16	78.3 \pm 4.2 *
Mitomycin C	13 (88 \pm 55)	13 (76 \pm 19)	113 \pm 14	90.8 \pm 5.9	14 (56 \pm 34)	14 (78 \pm 20)	106 \pm 16	81.7 \pm 6.8 *
Paclitaxel	13 (80 \pm 49)	13 (84 \pm 24)	44 \pm 13	72.7 \pm 6.5 *	12 (43 \pm 29)	12 (71 \pm 27)	63 \pm 9	49.9 \pm 5.0 *
Irinotecan	6 (73 \pm 42)	6 (94 \pm 18)	113 \pm 31	92.4 \pm 12.7	6 (14 \pm 7)	6 (93 \pm 14)	104 \pm 37	98.3 \pm 4.4
SN-38	3 (94 \pm 47)	3 (89 \pm 7)	69 \pm 44	54.8 \pm 26.8	5 (50 \pm 37)	5 (97 \pm 21)	108 \pm 42	60.1 \pm 14.4 *
BSP	14 (88 \pm 49)	14 (75 \pm 18)	44 \pm 18	36.1 \pm 4.1 *	14 (73 \pm 43)	14 (75 \pm 25)	117 \pm 5	35.0 \pm 4.2 *

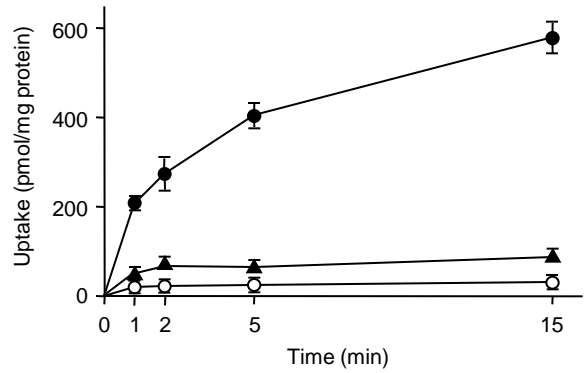
Fluorescence intensities were determined with the "Object Intensity Module" of the IN Cell Analyzer 1000. Each value represents the mean \pm S.E. except for "events" (mean \pm S.D.). "events" means cell numbers used for each experiment. * P < 0.05, significantly different from control.

Figure 1

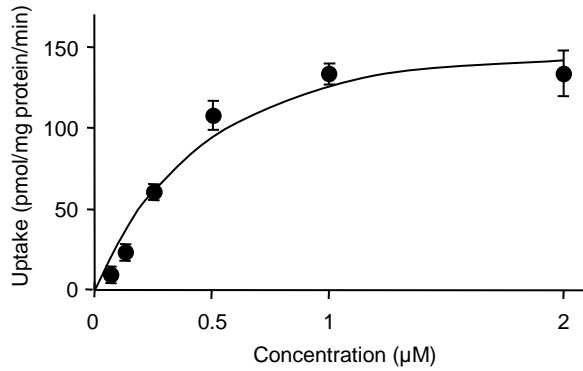
A



B



C



D

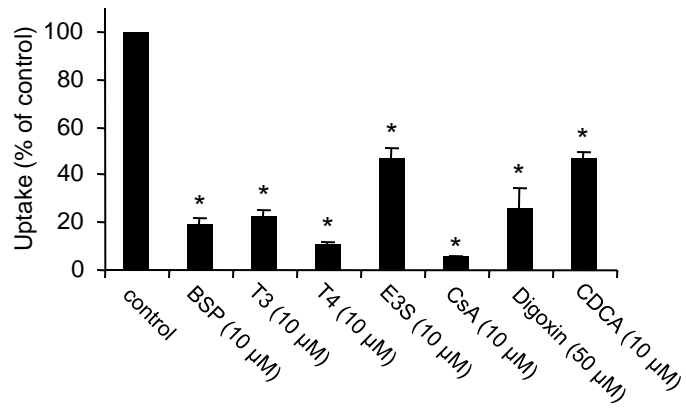


Figure 2

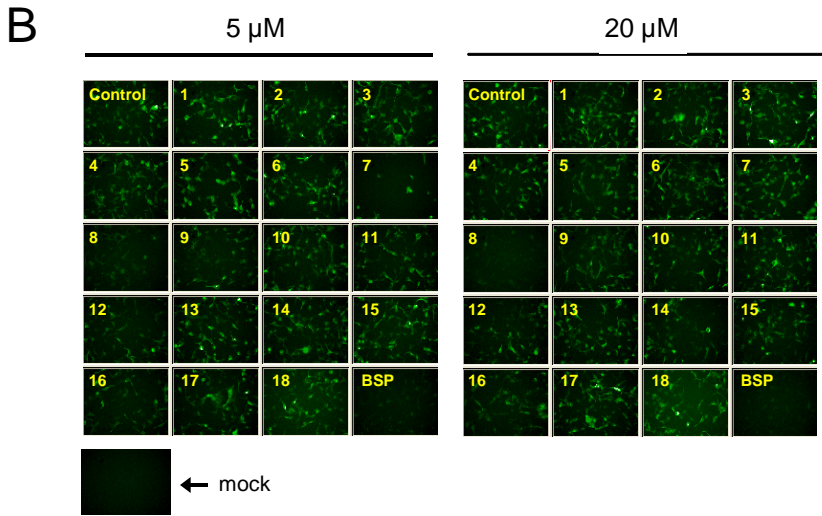
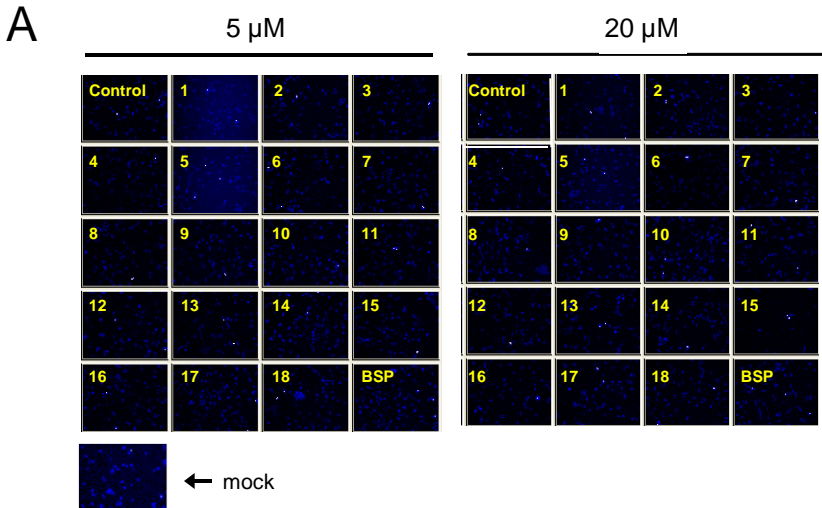


Figure 3

